UNIVERSITY OF CALIFORNIA SAN DIEGO

Cerebral Cavernous Malformation (CCM) Driven by Loss of Endothelial Krit1 is Exacerbated by Disruption of the Heart of Glass (Heg1) Receptor Pathway

A Thesis submitted in partial satisfaction of the requirements for the degree Master of Science

in

Biology

by

Jenny Lin

Committee in Charge:

Professor Alexandre Gingras, Chair
Professor Julian I Schroeder, Co-Chair
Professor Ashley Lauren Juavinett
Professor Amy Kiger

2021

The Thesis of Jenny Lin is approved, and it is acceptable in quality and form for publication on microfilm and electronically.

University of California San Diego

2021

DEDICATION

I dedicate this thesis to the fellow members of the Ginsberg Lab for their continuous guidance and support.

I'd also like to dedicate this thesis to my family. Thank you for your endless love and support.

TABLE OF CONTENTS

LIST OF FIGURES

LIST OF TABLES

ACKNOWLEDGEMENT

I would like to thank Dr. Gingras and Dr. Ginsberg for offering me the opportunity to study and work in the laboratory. Without their guidance, I could not have accomplished this thesis.

I would also like to thank Dr. McCurdy for being my mentor. Through multiple drafts and many long nights, her continuous support throughout the year has proved to be invaluable. I am deeply grateful for being her student. Her guidance has helped me overcome many adversities and become a better scientist.

I would also like to thank Dr. Schroeder, Dr. Juavinett and Dr. Kiger, who have kindly accepted to be part of my committee. I have gained valuable knowledge from their lectures, and they have inspired me greatly on my quest for completing my thesis.

This thesis contains unpublished materials preparing for publication co-authored with McCurdy, Sara; Gingras, Alexandre; and Ginsberg, Mark H. The thesis author will be an author of the paper.

ABSTRACT OF THE THESIS

Cerebral Cavernous Malformation (CCM) Driven by Loss of Endothelial Krit1 is Exacerbated by Disruption of the Heart of Glass (Heg1) Receptor Pathway

by

Jenny Lin

Master of Science in Biology

University of California San Diego, 2021

Professor Alexandre Gingras, Chair
Professor Julian I Schroeder, Co-Chair

Cerebral Cavernous Malformations (CCMs) are common vascular disruptions occurring mainly in the brain and spinal cord in which chronic hemorrhage leads to neurological deficits, headaches, seizures, and sometimes death. The 3 genes known to cause CCM when mutated include *Krit1* (Krev Interaction Trapped 1), *CCM2*, and *PDCD10* (Programmed Cell Death 10, also known as CCM3). Heg1 (Heart of Glass) is a transmembrane protein known to recruit and anchor both Krit1 and Rasip1 (Ras Interacting Protein 1) to the membrane, maintaining vascular homeostasis by stabilizing endothelial cell-cell junctions. It has been shown that endothelial deficiency of Krit1, CCM2, or PDCD10 will lead to CCM lesion formation in various mouse models. Interestingly, although deletion of Heg1 alone does not lead to CCM development, when Heg1 is deleted in combination with Krit1, lesions formation is exacerbated. Our task was to find the potential pathways Heg1 is involved in that lead to the exacerbation of CCM lesion

formation. Through *in vivo* and *in vitro* experiments, we found that when both Krit1 and Heg1 are depleted, lesion volume in mouse hindbrains increases, and Klf4 expression is drastically amplified in retinal endothelial cells. We found that Rasip1, an important Heg1 interactor, functions in the same pathway as Krit1 and Heg1. In addition, Mekk3 is important in the regulation of Klf2/4 expression, and knockdown of Mekk3 can rescue the increased Klf2/4 expression caused by Krit1/Heg1 knockdown. Further experiments are needed to better understand the role of Heg1 in the development of CCMs and elucidate the pathways involved.

INTRODUCTION

Cerebral Cavernous Malformations (CCMs) are common vascular malformations affecting an estimated 1 in 200 individuals (Leblanc et al., 2009). CCMs occur mainly in the brain and spinal cord, but also occasionally in the retina and skin. With leakage of blood into the surrounding tissue, and insufficient nutrients being transported throughout the brain and spinal cord, CCMs can lead to a wide range of neurological problems such as migraine-like headaches, seizures, and hemorrhagic stroke (Akers et al., 2017). Currently, there are no approved drug treatments for CCMs. Depending on the severity and the location of the lesions, surgical removal remains the primary option for CCM patients (Akers et al., 2017). Understanding the pathways involved in CCM pathogenesis may open new avenues for viable drug treatments in the future.

Endothelial cells make up the inner lining of all blood vessels and serve as a selective semipermeable barrier for transport of water, nutrients, and other molecules (Dejana 2004). Blood vessels are lined by a monolayer of endothelial cells and CCMs are characterized by dilated leaky blood vessels, resulting mainly from the disruption of proper endothelial cell-cell adhesion and dysfunctional angiogenesis (Padarti and Zhang 2018). Adhesion and contact between adjacent endothelial cells are mediated by intercellular junctions. Gap junctions, tight junctions, and adherens junctions are all forms of junctional complexes found in the endothelium.

Gap junctions are protein channels that allow the direct passage of small molecules between adjacent cells' cytoplasm. Tight junctions connect the extracellular domains of adjacent cells through transmembrane proteins and are critical in regulating the selective movement of solutes across the endothelium by forming a watertight seal between adjacent cells (Anderson and Itallie 2009). One important protein regulating tight junctions is ZO-1 (Zonula occludens-1,

also known as Tight junction protein-1), which is important for maintaining the blood-brain barrier within the central nervous system (Stevenson et al., 1986). Although tight junctions do provide some support in the attachment of adjacent cells, tight junctions are less resistant to mechanical stress than adherens junctions. Adherens junctions are primarily composed of cadherins and catenins (Guo et al., 2007). The extracellular portion of a cell's cadherin binds to the extracellular portion of another cell's cadherin. The intracellular tail of cadherin is anchored to the cell's internal cytoskeleton (actin filaments) through catenins, providing strong adhesion between adjacent cells (Guo et al., 2007). The functional status of adherens junctions contributes to the control of vessel morphogenesis and cell migration, playing a vital role in angiogenesis -- the development of new blood vessels (Petzelbauer et al., 2000). VE-cadherin (vascular endothelial cadherin) is the main cadherin protein for maintaining the endothelial barrier integrity (Giannotta et al., 2013). Insufficient expression of VE-cadherin is linked to the disruption of vascular integrity and the development of CCMs, and the restoration of VE-cadherin expression has shown to reduce both the vascular leakage in lesions and the size of established lesions in mouse hindbrain (Li et al., 2020).

The molecular pathway involved in the development of CCMs can be attributed to the loss-of-function mutations in genes encoding Krit1 (Krev Interaction Trapped 1, also known as CCM1, Cerebral Cavernous Malformation-1), CCM2 (also known as Malcaverin), or PDCD10 (Programmed Cell Death 10, also known as CCM3) (Chan et al., 2010). The three CCM proteins can form a trimeric complex and are involved in a wide range of signaling pathways. The localization of the complex to endothelial cell-cell junctions is necessary to maintain the structural integrity of the vasculature (Draheim et al., 2014). Depletion of endothelial Krit1 causes β-catenin to dissociate from VE-cadherin, resulting in disruption of adherens junctions

and subsequent increase in blood vessel permeability (Glading and Ginsberg 2010). A novel type I transmembrane protein receptor Heg1 (Heart of Glass) recruits and anchors both Krit1 and Rasip1 (Ras Interacting Protein 1) at endothelial junctions to ensure stable cell-cell adhesions (De Kreuk et al., 2015).

As indicated in Figure 1b, alterations to the CCM molecular pathway dramatically changes the expression levels of downstream proteins. Loss of Krit1 leads to the loss of CCM complex, and downstream activation of MEKK3 (Mitogen-activated protein kinase kinase kinase 3), a protein that is normally inhibited by the Krit1/CCM2 complex in endothelial cells (Zhou et al., 2015). Activation of MEKK3 increases the expression of the transcription factors Klf2 and Klf4, which has been identified as a key driver of CCM development (Li et al., 2020). Given that Heg1 is known to regulate vascular homeostasis, we hypothesized that the simultaneous loss of *Krit1* and *Heg1* in a mouse model will have a detrimental effect on CCM lesion formation. Furthermore, we predict that endothelial cells *in vitro* would lead to compromised cell-cell junctions (adherens junctions specifically) and increased activation of the Mekk3 pathway upon simultaneous knockdown of *Krit1* and *Heg1*.

RESULTS

It is well established that endothelial specific deletion of *Krit1* leads to the development of CCM lesions in a neonatal mouse model of the disease (Zheng et al., 2014). To compare lesion burden in mouse hindbrain when 1 or both copies of *Heg1* are deleted on a *Krit1* ECKO (endothelial cell knockout) background, two genetic mouse strains were utilized. Due to the embryonic lethality of Krit1 loss, the cre-lox system was used to temporally control expression of *Krit1* and/or *Heg1*, two genes encoding proteins of the CCM complex. A tamoxifen-inducible Cre recombinase (iCre-ERT2) driven by the Pdgfb promoter was used to specifically target endothelial cells. Deletion of *Krit1* alone or in combination with one or both alleles of *Heg1* at postnatal day 1 leads to the development of CCM brain lesions by postnatal day 7-9. Brightfield images of representative brains from postnatal day 8 mice were taken (Fig. 2A). Lesion volume was quantified using microCT scanning and was normalized to total brain volume (Fig. 2B). When both copies of *Krit1* are deleted, blood-filled CCM lesions in the hindbrain can be observed in red (Fig. 2A). *Heg1* deletions by itself did not result in any lesions (Fig. 2). Lesion volume in the mouse hindbrain increased with the deletion of 1 or both copies of *Heg1* on a *Krit1* ECKO background, covering larger areas and appearing darker in color, and was further confirmed through the quantification of lesion volume (Fig. 2). Normalized lesion volume for each condition was compared to Cre-negative control and data was analyzed using one-way ANOVA with Bonferroni post-test (* $p < 0.05$; ** $p<0.01$; *** $p < 0.001$).

Excess expression of Klf4 correlates to an increase in lesion formation and worsened CCM development (Li et al., 2020). To investigate the potential mechanism of increased lesion burden when *Heg1* is deleted on the *Krit1* ECKO background, we measured the nuclear expression of Klf4 protein in mouse retinas by immunohistochemistry and confocal microscopy.

Cre-negative mice were used as negative controls. Klf4 immunostaining appeared brighter when 1 or both copies of *Heg1* are deleted compared to *Krit1* ECKO alone, and all conditions were brighter than Cre-negative controls (Figure 3A). Expression was quantified by measuring the integrated density of nuclear localized Klf4 staining (RFU/nucleus; Relative Fluorescence Units/nucleus; ImageJ). There was an observable trend towards increasing Klf4 expression comparing Cre-negative controls, $Krit1^{F/F}$, $Krit1^{F/F}$;$Heg1^{F/+}$ and $Krit1^{F/F}$;$Heg1^{F/F}$ mouse retinas (Fig. 3B). Using one-way ANOVA, Klf4 expression was statistically significantly higher in $Krit1^{F/F}$;$Heg1^{F/+}$ retinas and $Krit1^{F/F}$;$Heg1^{F/F}$ retinas compared to controls (***, $p < 0.001$; Fig. 3B).

To further investigate the effects of knocking down *Krit1*, *Heg1*, and the combination of the two genes on the expression of Klf2/Klf4, *in vitro* experiments were conducted using human umbilical vein endothelial cells (HUVECs). siRNA was used to knockdown gene expression of *Krit1* and *Heg1* individually, or in combination. Fold change was calculated using the delta-delta Ct method (also known as the $2^{-\Delta\Delta Ct}$ method) and normalized to the expression of the housekeeping gene, GAPDH (Glyceraldehyde 3-phosphate dehydrogenase). The efficiency of knockdowns was first confirmed using quantitative reverse transcriptase (qRT)-PCR (Fig. 4A, B). *Heg1* expression increased when *Krit1* was knocked down (** $p < 0.01$, Fig. 4B). Both *Krit1* and *Heg1* knockdown individually led to increased *Klf2/Klf4* transcript, and the effect was further amplified following *Krit1/Heg1* double knockdown (Fig. 4C, D). For Klf4 expression specifically, a synergistic amplification was detected with *Krit1/Heg1* double knockdown (*** $p < 0.001$ by ANOVA test; Fig. 4D). This synergistic increase may partially explain the significantly larger lesion volume found in *Krit1/Heg1* double ECKO mice (Fig. 2).

The effects of *Heg1* depletion on a *Krit1* ECKO mouse background regarding the cellular structure integrity was also investigated *in vitro* using HUVECs. siRNA pools targeting Krit1 and Heg1 mRNA were used to deplete gene expression. Phalloidin staining of F-actin (filamentous actin) was utilized to evaluate the status of endothelial cell structure and cell-cell attachment. *Krit1* and *Heg1* knockdowns individually resulted in a mild disruption of F-actin (Fig. 5A). Cellular structure was further compromised with the double knockdown of *Krit1* and *Heg1*, leading to an increase in F-actin disruption and an increase in endothelial cell detachment (Fig. 5A). Acellular area was quantified and measured as DAPI-negative percent of total area (ImageJ, Fig. 5B). A significant decrease in endothelial cell coverage was detected with *Krit1/Heg1* double knockdown (***, $p < 0.001$; Fig. 5B).

The membrane-localization of the CCM complex is required for the stabilization of VE-cadherin, maintaining vascular integrity (Petzelbauer et al., 2000). Insufficient expression of VE-cadherin is linked to the disruption of cell-cell adhesion and increased vascular permeability (Li et al., 2020). Therefore, HUVECs treated with siRNAs underwent immunostaining for VE-cadherin and ZO-1. *Heg1* knockdown cells appeared to undergo morphological changes and took on a more elongated shape (Fig. 5C). Cells with *Krit1/Heg1* double knockdown had severely compromised adherens junctions while showing the elongated phenotype, and some cells appeared to have dysfunctional cell division, possibly due to the disruptions in cytoskeletal integrity (white circle indicating a cell with multiple nuclei; Fig. 5C). VE-cadherin expression and ZO-1 expression were quantified using ImageJ. Cells with *Krit1* single knockdown showed a significant decrease in VE-cadherin expression compared to scrambled controls; an amplified reduction in VE-cadherin expression was detected with *Krit1/Heg1* double knockdown (**, $0.001 < p < 0.01$; ***, $p < 0.001$; data analyzed by one-way ANOVA; Fig. 5D). While significant

reductions in ZO-1 expressions were recorded across all conditions (*Krit1, Heg1* single knockdowns and *Krit1/Heg1* double knockdown), *Krit1/Heg1* double knockdown compromised ZO-1 expression to a greater extent compared to *Krit1* knockdown alone (**, $0.001 < p < 0.01$; ***, $p < 0.001$; data analyzed by one-way ANOVA; Fig. 5E).

Given that Heg1 regulates the localization of Rasip1 (De Kreuk et al., 2015), a protein that helps stabilize VE-cadherin at the membrane, we next sought to determine whether Rasip1 was also involved in the Krit1/Heg1 phenotypes we previously observed. The effects of *Rasip1* knockdown on the expression of *Klf2/4* were evaluated in HUVECs. As previously shown in Figure 4, *Krit1/Heg1* double knockdown cells again showed significantly amplified *Klf2/4* expressions (Fig. 6A, B). Interestingly *Rasip1/Krit1* double knockdown upregulates *Klf2/4* to a similar extent as *Krit1/Heg1* double knockdown (Fig. 6A, B). In addition, *Klf4* expression showed no significant differences between *Krit1* and *Heg1* single knockdown cells, as well as *Rasip1/Heg1* double knockdown cells (Fig. 6B). The results suggest that Rasip1 and Heg1 are likely in the same pathway, since the combination knockdown of either gene (*Heg1* and *Rasip1*) with Krit1 leads to a similar upregulation of Klf2/Klf4, while the combination of Heg1/Rasip1 does not (Fig. 6A, B).

In a separate siRNA experiment, also conducted in HUVECs, *Mekk3* was knocked down as an attempt to rescue the increase in *Klf2/4* expression in *Krit1/Heg1* double knockdown cells. The amplified expression of *Klf2* caused by *Krit1*, *Heg1*, or the *Krit1/Heg1* combination knockdown were successfully rescued by depleting *Mekk3* (* $p < 0.05$; ** $p < 0.01$; Fig. 6C). *Klf4* expression was also successfully rescued by knocking down *Mekk3*, except in *Heg1* knockdown cells (* $p < 0.05$; Fig. 6D).

FIGURES

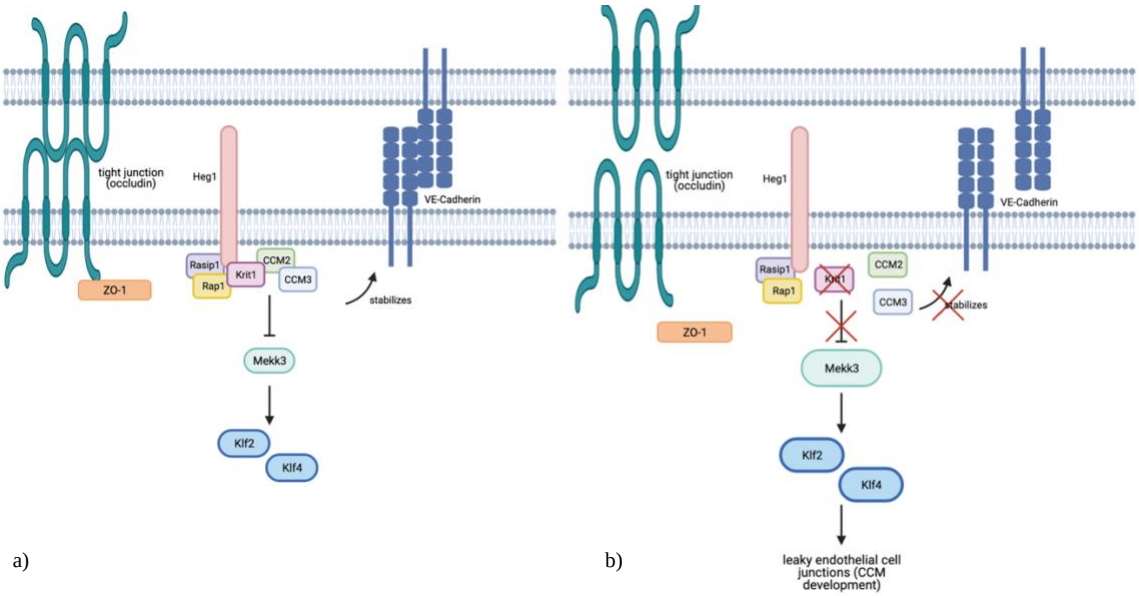

Figure 1. The molecular pathway involved in CCM development. (a) A properly functioning CCM pathway is essential to the inhibition of MEKK3 activity and limiting the expression of transcription factors Klf2 and Klf4, ensuring the stability of cell-cell adhesion and vascular integrity; (b) Loss of Krit1 results in the loss of CCM complex, leading to an increase in Klf2 and Klf4 signaling and destabilization of endothelial cell junctions.

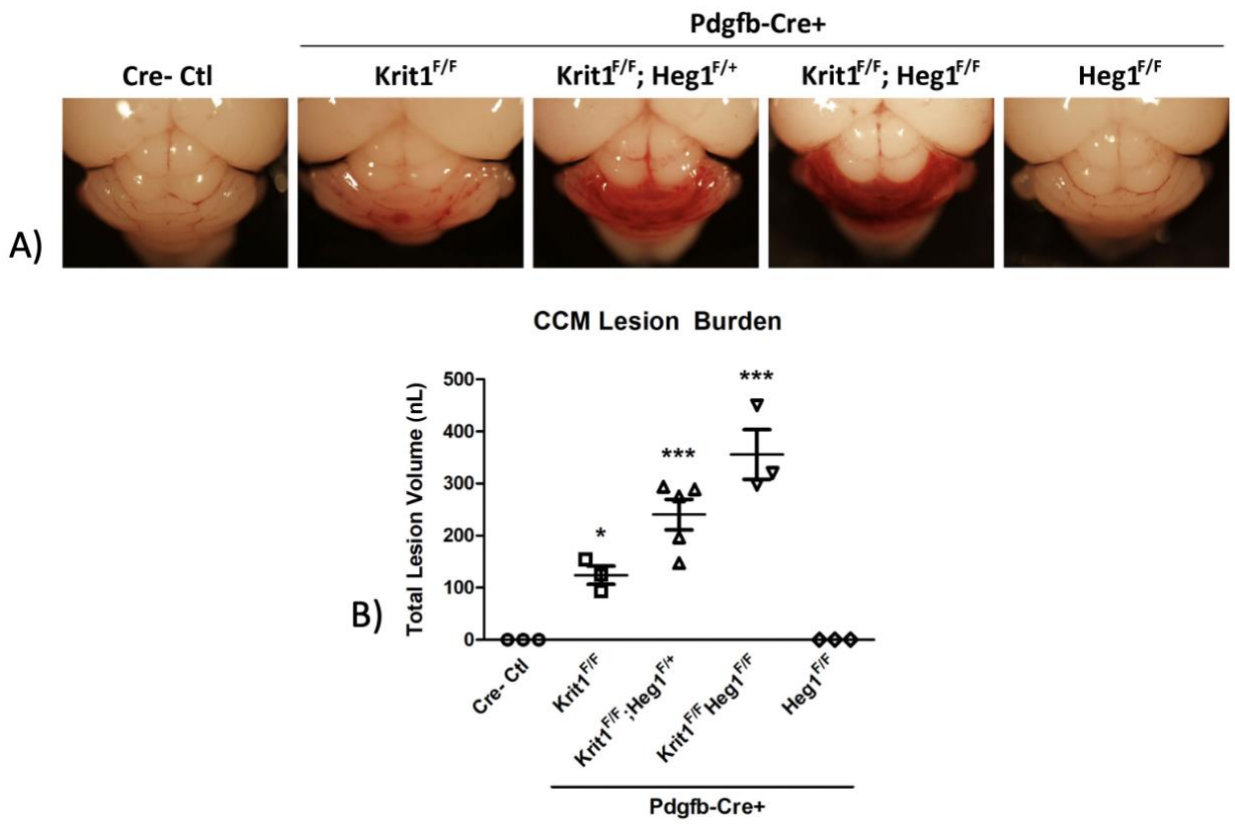

Figure 2. Deletion of *Heg1* alleles on a *Krit1* ECKO background increases lesion burden in the mouse hindbrain. (A) Brightfield images of representative brains from postnatal day 8 mice are shown for each condition (Cre-negative control, $Krit1^{F/F}$, $Krit1^{F/F}$;$Heg1^{F/+}$, $Krit1^{F/F}$;$Heg1^{F/F}$, and $Heg1^{F/F}$). Blood-filled CCM lesions are visible in three of the conditions ($Krit1^{F/F}$, $Krit1^{F/F}$;$Heg1^{F/+}$, and $Krit1^{F/F}$;$Heg1^{F/F}$). (B) Lesion volume was measured by microCT and normalized to total brain volume, expressed in nanoliters (nL). F denotes a floxed allele, while + represents a wild type allele. Pdgfb-Cre is a Cre-recombinase driven by the Pdgfb promoter. Data analyzed by one-way ANOVA with Bonferroni post-test. * $p < 0.05$; ** $p < 0.01$; *** $p < 0.001$.

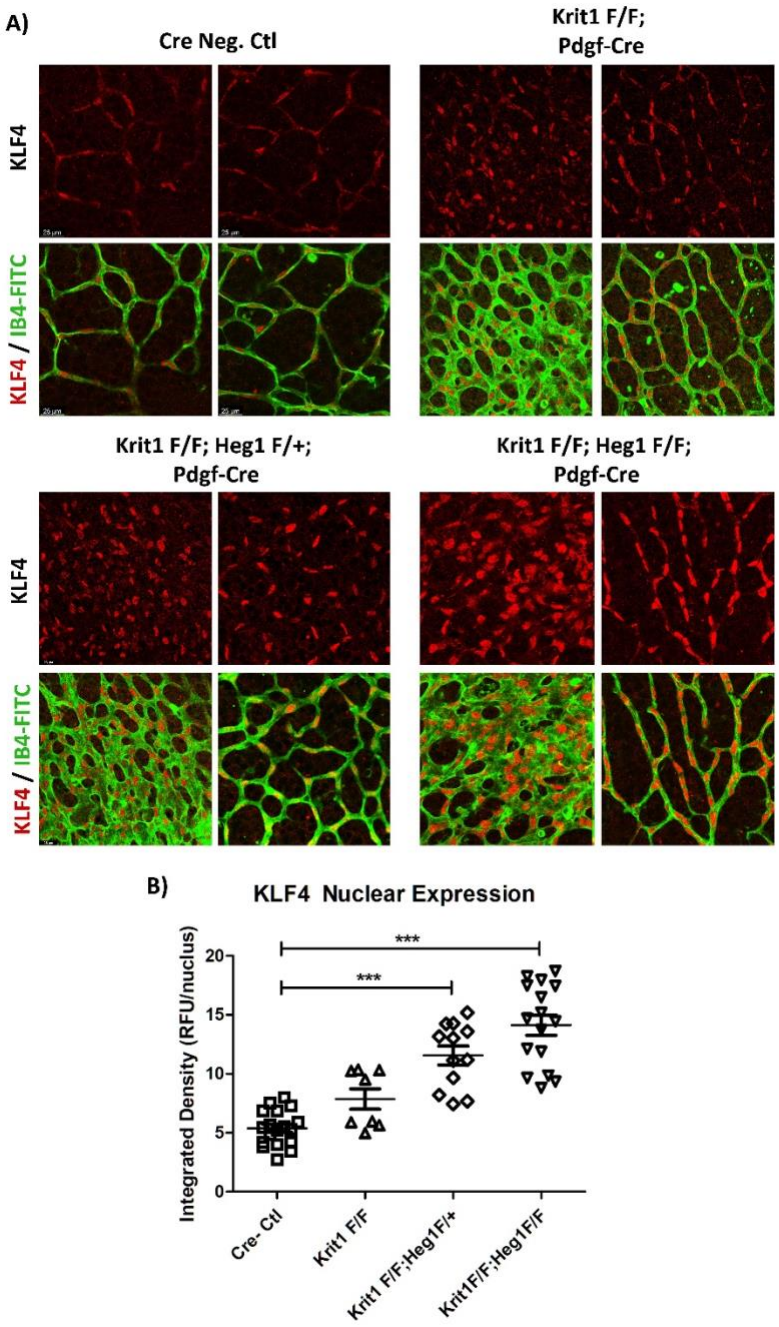

Figure 3. Deletion of *Heg1* alleles on a *Krit1* ECKO background increases nuclear Klf4 expression in mouse retinas. (A) Detection of Klf4 expression by immunostaining using Klf4 antibody (red). Isolectin B4-FITC (IB4-FITC) was used to identify blood vessels (green). (B) Klf4 expression was quantified using integrated density (RFU/nucleus; Relative Fluorescence Units/nucleus; ImageJ). When one or both copies of *Heg1* were depleted on a *Krit1* ECKO background, Klf4 expression in nuclei increased significantly compared to Cre-negative control. Data analyzed by one-way ANOVA with Bonferroni post-test. * $p < 0.05$; ** $p < 0.01$; *** $p < 0.001$.

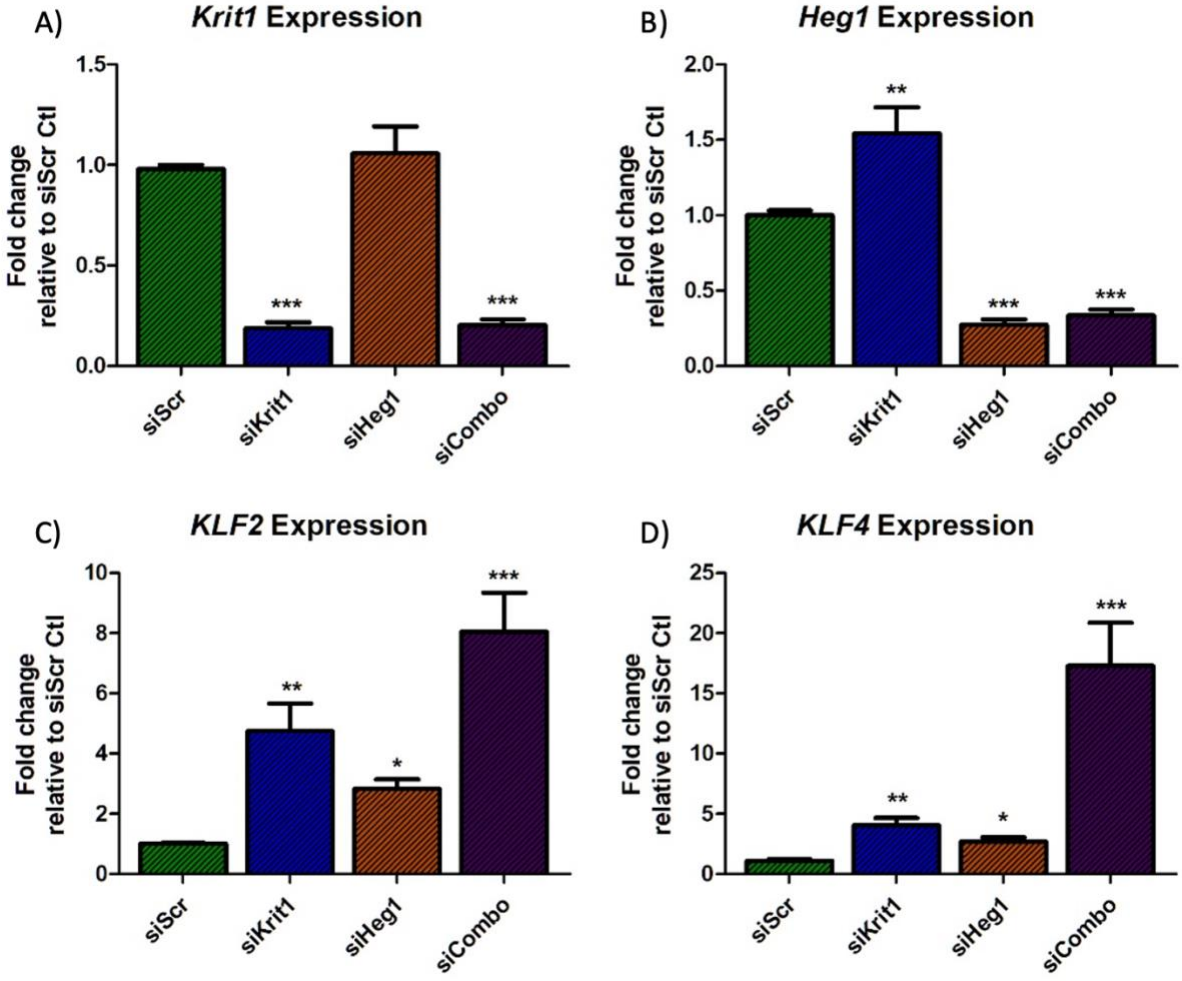

Figure 4. Depletion of both *Krit1* and *Heg1* results in significant increase of *Klf2* and *Klf4* expression *in vitro.* Data collected using quantitative PCR, which measures the amount of specific RNA transcripts in the cell and compares the amplification of the targeted genes. (A & B) The qPCR graphs confirm that the *Krit1* knockdown cells have a significantly lower expression of *Krit1* gene, and the *Heg1* knockdown cells have a lower expression of *Heg1* gene. Knock down of both genes in combination (siCombo) is also effective. (C & D) Expression of Klf2 and Klf4 are increased upon knockdown of *Krit1* or *Heg1* alone, while the effect is further amplified when both Krit1 and Heg1 are knocked down (siCombo). Data analyzed by one-way ANOVA, * $p < 0.05$; ** $p < 0.01$; *** $p < 0.001$.

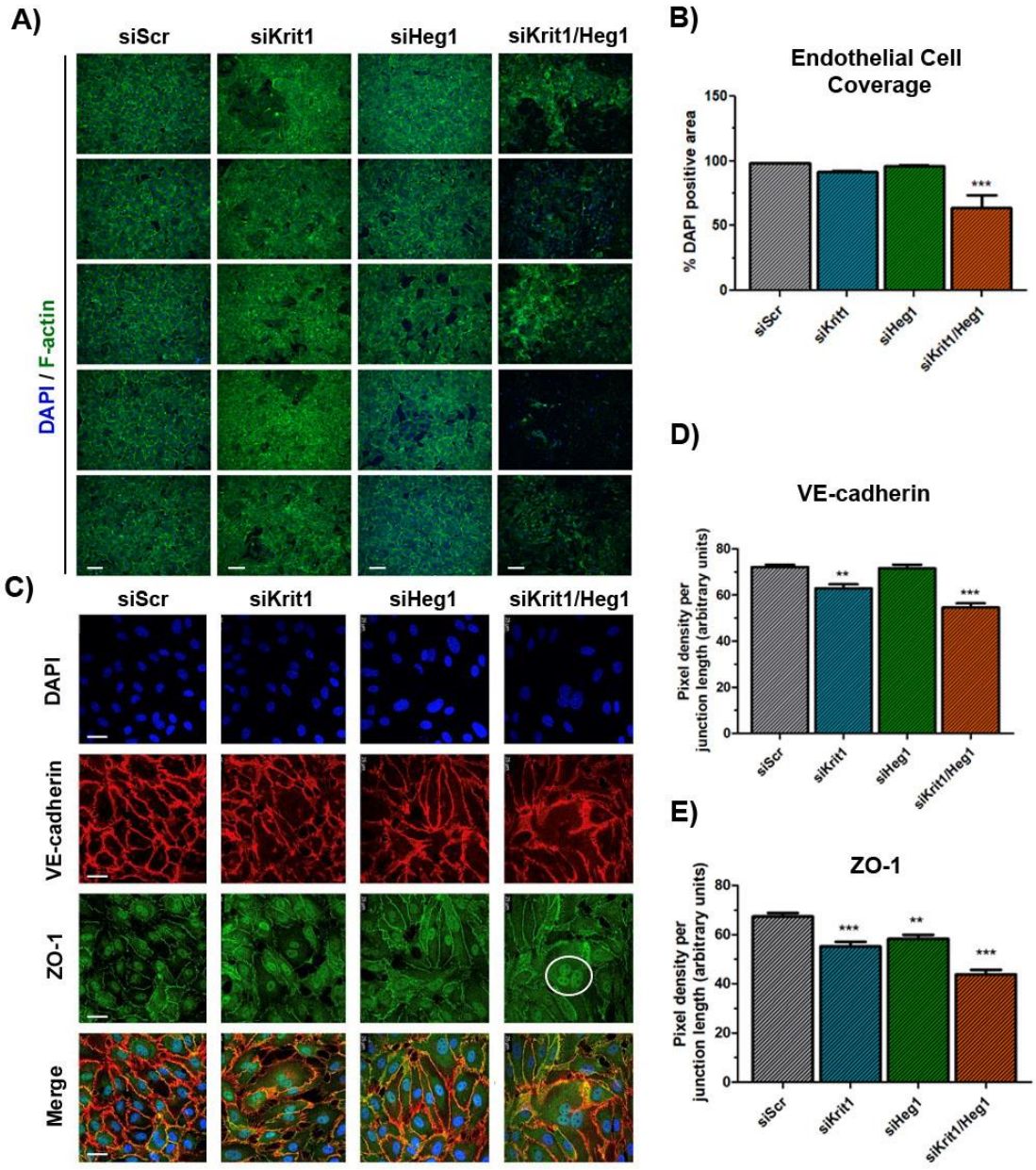

Figure 5. Knockdown of *Krit1* and/or *Heg1* leads to endothelial cell detachment, and disrupted junction protein localization *in vitro*. (A) Phalloidin staining of F-actin (filamentous actin). siRNA transfection with Lipofectamine was utilized to deplete mRNA levels of Krit1 and Heg1. Non-targeting scrambled siRNA was used as negative control. Dark spots indicate the disruption in F-actin. (B) Quantification of acellular area, measured as DAPI-negative percent of total area. Scale bar = 200µm. (C) Immunostaining for DAPI, VE-cadherin and ZO-1. White circle indicates an observation of dysfunctional cell division when both Krit1 and Heg1 were depleted. (Scale bar = 25 µm. (D) Quantification of VE-cadherin expression was performed using ImageJ by measuring pixel intensity along cell-cell junctions. (E) Similar analysis for ZO-1 junctional expression was performed using ImageJ. Data analyzed by one-way ANOVA with Bonferroni post-test. ** $p < 0.01$; *** $p < 0.001$.

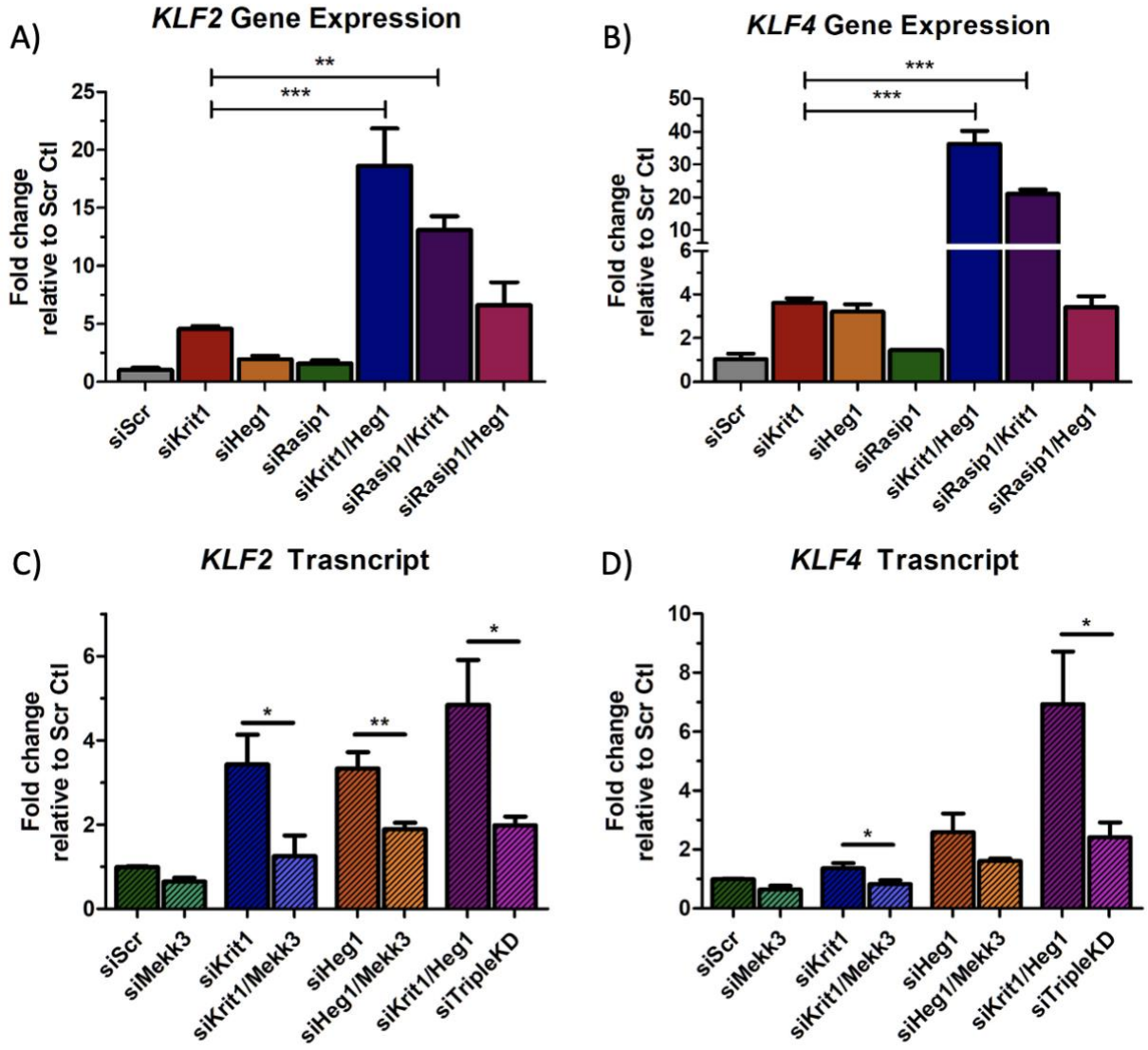

Figure 6. Knockdown of *Krit1*, in combination with either *Heg1* or *Rasip1*, upregulates *Klf2* and *Klf4* to a similar degree, while *Mekk3* depletion partially rescues *Klf2* and *Klf4* levels. HUVECs were cultured and treated with siRNAs to deplete specific gene transcripts. (A & B) Effects of Rasip1 knockdown was investigated. *Krit1/Rasip1* knockdown upregulated *Klf2/4* to a similar extent as *Krit1/Heg1* knockdown. Data analyzed by one-way ANOVA with Bonferroni post-test. (C & D) *Mekk3* was knocked down to determine its effects on *Klf2/4* upregulation. Triple knockdown of *Krit1*, *Heg1*, and *Mekk3* showed a significant decrease in both *Klf2/4* expressions compared to *Krit1/Heg1* knockdown. Data analyzed by one-way ANOVA with Bonferroni post-test. * $p < 0.05$; ** $p < 0.01$; *** $p < 0.001$.

DISCUSSION

The development of Cerebral Cavernous Malformation (CCM) is tightly linked to the loss-of-function mutations in genes encoding Krit1, CCM2 and PDCD10 (Chan et al., 2010). In preliminary studies investigating the molecular pathway of CCM development, Heg1, a novel type I transmembrane protein, has been shown to play an important role by recruiting and anchoring Krit1 and Rasip1 at endothelial junction, stabilizing the monolayer (De Kreuk et al., 2015). Through the experiments described in detail above, we have discovered that loss of Heg1 exacerbates the pathogenesis of Krit1-driven CCM phenotypes *in vitro* and *in vivo*. Therefore, we conclude that the Heg1 molecular pathway is worth further investigation in the context of Krit1-driven CCM development and endothelial homeostasis.

To initially investigate the effects of *Heg1* deletion on a *Krit1* ECKO (endothelial cell knockout) background we crossed mice with *Krit1* and *Heg1* floxed alleles, with a tamoxifen-inducible Cre driven by the endothelial specific promoter, Pdgfb. CCM lesion development in the hindbrain was visible 8 days after gene deletion. Brightfield images of representative brains revealed a stark increase in blood-filled lesions when both *Krit1* and *Heg1* (one or both alleles) were deleted compared to *Krit1* deletion alone (Figure 2A). Following microCT analysis of the same brains, we observed that the hindbrain lesion volume was significantly increased with the deletion of 1 or both copies of *Heg1* in a dose-dependent manner (Fig. 2B). This result was surprising, as it is known that *Heg1* deletion alone does not lead to formation of lesions in the hindbrain (Zheng et al., 2014). It should be noted that *Heg1* KO mice did show defective lymphatic vessel junction assembly (Kleaveland et al., 2009), even though blood vessel endothelial cells appear unaffected. While Heg1 is known to bind and stabilize Krit1 at EC junctions, if the involvement of Heg1 within the CCM molecular pathway is restricted to its

association with Krit1, then Heg1 depletion should not exacerbate the development of lesions caused by the loss of Krit1. The worsened lesions suggest that Heg1 may affect other signaling pathways in addition to those directly regulated by Krit1.

For that reason, we examined the effects of *Heg1* depletion on two downstream transcription factors important for endothelial monolayer homeostasis, Klf2 and Klf4. Endothelial Klf2/4 control a large portion of the endothelial transcriptome and are crucial in maintaining vascular integrity (Sangwung et al., 2017). Upregulation of Klf2/4 is a known driver in the development of CCM (Li et al., 2020), and genetic deletion of either *Klf2* or *Klf4* on a *Krit1* ECKO mouse background significantly reduces lesion development (Zhou et al., 2016). We harvested mouse retinas from P8 neonatal mice (Cre-negative control., $Krit1^{F/F}$; $Krit1^{F/F}/Heg1^{F/+}$; or $Krit1^{F/F}/Heg1^{F/F}$) and detected Klf4 expression by immunostaining (Fig. 3A). Fluorescent images revealed that the deletion of both *Krit1*and *Heg1* resulted in amplified Klf4 expression compared to retinas with *Krit1* deletion alone (Fig. 3B). The upregulation of Klf4 could potentially explain the observed increase in lesion volume by compromising vascular integrity and destabilizing cell-cell adhesion.

Experiments were then conducted *in vitro* using HUVECs and siRNA to evaluate the relationship between *Krit1/Heg1* expression and *Klf2/4* expression in endothelial cells. While *Krit1* knockdown alone led to an increase in *Klf2/4* transcript, *Krit1/Heg1* double knockdown further upregulated the expression of *Klf2* (Fig. 4C). Interestingly, in contrast to a more linear increase in Klf4 expression as observed through *in vivo* experiments, a synergistic increase in *Klf4* expression was detected *in vitro* following *Krit1/Heg1* double knockdown (Fig. 4D). A potential explanation would be the complicated nature of the *in vivo* microenvironment, as well as the difference in measuring *Klf2/4* transcript *in vitro* and Klf4 protein *in vivo.* Further

investigations are needed to explain the differences between *in vivo* and *in vitro* findings. Nonetheless, through both experiments, it can be concluded that the amplified upregulation of Klf4 may partially explain the significantly larger lesion volume found in *Krit1/Heg1* double ECKO mice.

The effects of *Krit1* and/or *Heg1* knockdown on endothelial cell junctions were also examined using immunostaining of HUVECs. With single knockdowns of *Krit1* or *Heg1*, the cells exhibited morphological changes where they became more elongated (Fig. 5C), appearing to have lost cytoskeletal structure. The localization of F-actin (actin filaments), VE-cadherin and ZO-1 were disrupted with the depletion of *Krit1* or *Heg1*, and the effects were magnified in double knockdown cells (Fig. 5C, D, E). As mentioned previously, it is known that Heg1 binds and localizes Krit1 to cell membrane, enabling Krit1 to stabilize VE-cadherin and ensuring the functionality of adherens junctions, which are essential in supporting the cell-cell adhesion's resistance to mechanical stress (Glading and Ginsberg 2010). Upon loss of *Krit1* or *Heg1*, we observe a mild destabilization of VE-cadherin from junctions, resulting in the disruptions of cell-cell adhesion. This would imply that loss of either protein alone, might still allow some compensatory mechanism for maintaining endothelial cell junction stability. However, when both *Krit1* and *Heg1* are depleted from HUVECs, we observe a significantly larger affect. Since adherens junctions are formed through the interactions between VE-cadherins and the cytoskeleton (Giannotta et al., 2013), which consists of actin filaments, it is possible that with dysfunctional adherens junctions, the cellular structure maintained by F-actin is also negatively affected. It is likely that the weakened adherens and tight junctions, as well as disruption in cytoskeletal structure, undermine vascular integrity, ultimately resulting in worsened lesion formations *in vivo*.

To further understand the potential signaling pathways involved in the phenotypes we observed *in vitro*, the role of Rasip1, a binding partner of Heg1, was examined. Based on previous studies, increase in Rho-associated protein kinase (ROCK) activity contributes to CCM development by increasing the cell's actomyosin contractility and stress fiber formation (Draheim et al., 2014). Rasip1 interacts with RhoA GTPase activation protein, ARHGAP29, to suppress ROCK activity (Su and Calderwood 2020). Heg1 recruits Rasip1 to the endothelial membrane where it can be found at cell-cell junctions. Loss of Heg1 prevents the stabilization of Rasip1, and thereby leads to increased ROCK activity, resulting in the formation of stress fibers, adversely affecting vascular integrity (Su and Calderwood 2020).

We investigated the effects of *Rasip1* knockdown alone, and the depletion of *Rasip1* in combination with either *Krit1* or *Heg1* knockdown on the expression of *Klf2/4* (Fig. 6A, B). *Rasip1/Krit1* double knockdown upregulates *Klf2/4* to a similar extent as *Krit1/Heg1* double knockdown, suggesting Rasip1 to be in the same signaling pathway as Heg1 (Fig. 6A, B). *Klf4* expression showed no significant differences between *Krit1* and *Heg1* single knockdown cells, as well as *Rasip1/Heg1* double knockdown cells (Fig. 6B). This further confirms the speculation that Rasip1 is part of the same molecular pathway as Heg1.

Based on previously published studies, an intact and correctly localized CCM complex inhibits the activity of Mekk3, which is a key driver in the upregulation of Klf2/4 (Li et al., 2020). We hypothesized that by knocking down *Mekk3*, *Klf2/4* expressions could potentially be downregulated and rescued. The amplified expression of *Klf2/4* caused by *Krit1/Heg1* single and double knockdowns was successfully suppressed when *Mekk3* expression was depleted (Fig. 6C, D). This result indicates that the upregulation of *Klf2/4* upon loss of *Krit1/Heg1* is driven at least in part through the Mekk3 pathway. The difference in the fold change of *Klf2* and *Klf4*, as well

as the ability of *Mekk3* knockdown to rescue expression levels of each, suggests a potential divergence in the individual upstream regulators of Klf2 and Klf4. It is also possible that the interaction between Heg1 and Krit1 plays a major role in modulating Klf4 activity, but the control of *Klf2* expression also depends on the presence of other endothelial proteins. Alternatively, it may also be related to the fact that the expression of *Klf4* is much lower than that of *Klf2's* under normal conditions (as observed by absolute Ct values by qPCR, data not shown).

Taken together, these data reveal a previously unknown role of Heg1 in CCM development. The loss of Heg1 exacerbates the pathogenesis of Krit1-driven CCM, warranting further investigation of the various players in each pathway, especially those that overlap, such as the link between Rasip1 and the CCM complex, as well as Mekk3 driven expression of Klf2 and Klf4. There appears to be compensatory mechanisms that may stabilize Krit1 in the absence of Heg1. However, when both proteins are missing, endothelial dysfunction and CCM development is dramatically enhanced. The Heg1 molecular pathway should be investigated further to elucidate its role in CCM development and endothelial homeostasis.

MATERIALS AND METHODS

Antibodies and reagents

Name	Company	Catalog Number	Dilution
Goat-α-Mouse KLF4 primary anitbody	R&D Systems	AF3158	1:80 (2.5µg/mL)
Isolectin B_4-FITC	Sigma	L2895	1:50 (20ug/mL)
Goat-α-Human VE-cadherin	R&D Systems	AF938	1:50 (4µg/mL)
Rabbit-α-Human ZO-1	ThermoFisher Scientific	61-7300	1:50 (5µg/mL)
Phalloidin-AlexaFluor488	ThermoFisher Scientific	A12379	1:40 (5U/mL)
Donkey-α-Goat AlexaFluor-647 2'Ab	ThermoFisher Scientific	A-21447	1:300
Donkey-α-Rabbit AlexaFluor-488 2'Ab	ThermoFisher Scientific	A-21206	1:300
DAPI Fluormount G mounting medium	Southern Biotech	0100-20	N/A
Paraformaldehyde	Sigma	158127	4%, 2% w/v
Triton X-100	Calbiochem	9002-93-1	1% v/v
Bovine serum albumin	Sigma	A7030	1% w/v

qPCR Primers

Gene Name	Forward Primer 5'→3'	Reverse Primer 5'→3'
GAPDH	GGGCCATCCACAGTCTTCTG	CTCCTGCACCACCAACTGCT
KRIT1	CCATCGTACCTGTTACCAAACT	ACTGACACCTTCACTTGTACTG
HEG1	ACTGCCCGGATCGAGACAC	GCTCCCTTTTGGGGGTGTAGT
KLF2	AGACCACGATCCTCCTTGA	TCACAAGCCTCGATCCTCTA
KLF4	GGTCTGTGACTGGATCTTCTATC	ACCCTGATATCCACAACTTCC

Mouse models

All animal experiments were approved by the Institutional Animal Care and Use Committee (IACUC) of the University of California, San Diego, and were conducted following federal regulations as well as institutional guidelines and regulations on animal studies. Genetic mouse strains were made using a tamoxifen-inducible Cre-lox system driven by the endothelial promoter Pdgfb to delete *Krit1* and/or *Heg1*. A single intra-gastric injection of 4-hydroxy-tamoxifen dissolved in corn oil (50μg) was made per mouse at postnatal day 1 to induce gene deletion. Animals were sacrificed at postnatal day 8 for tissue collection and analysis.

Brain and retina collection

After CO_2 administration to euthanize the mice, postnatal day 8 pups were decapitated using sterile surgical scissors. A midline incision in the skin of the head was made starting from the posterior side and ending between the eye sockets. The skin was then folded over the eyes to below the jaw and held together using one hand for stability. A curved forceps was used to gently push the eye out of its socket and lifted from below into a collection tube containing 2% PFA, and fixed overnight before being transferred to 1X PBS. To collect the hindbrain tissues, a pair of curved scissors was used to cut across the nasal bridge, between the two eye sockets. Then, an incision was made on each side from the outer corner of the eye socket to the parietal lobe, along the horizontal plane. Two more cuts were made from the posterior side (entering from the brainstem) to ensure clear detachment between the superior and inferior portions. Using a pair of small, straight scissors, a midline cut was carefully made from the nasal bridge to the end of the frontal lobes. Forceps were then used to remove the skull in an anterior to posterior

manner. Lastly, a flat spatula pre-wetted in 4% PFA was used to remove and collect the brain, which was fixed in 4% PFA overnight.

Retina dissection and immunostaining

Following overnight fixation in 2% PFA, retinas were dissected from whole mouse eyes using forceps and small dissection scissors under a stereomicroscope. First, the cornea, iris, and pigmented epithelium were removed. Next the lens, along with hyaloid vessels, were removed from the remaining retina using forceps. The isolated retinas were then washed in PBS and incubated overnight in blocking buffer (1X PBS, 1% bovine serum albumin (BSA), 0.5% Triton X-100). Next retinas were incubated overnight at room temperature with primary antibody against KLF4 protein (R&D Systems, AF3158) diluted in 1% BSA in PBS. The retinas were then moved to 4ºC for an additional 48 hours. Next, the retinas were washed in PBS 3 times, 5 minutes each, followed by 3 more washes in PBlec buffer (1X PBS, 1mM $CaCl_2$, 1mM $MgCl_2$, 0.1mM $MnCl_2$, 1% Triton X-100). Retinas were then stained with Isolectin B4 diluted in PBlec

Cell transfection (siRNA transfection)

Before transfecting with siRNAs, Human umbilical vein endothelial cells (HUVECs) were seeded and grown to 70-90% confluence on plates coated with fibronectin (2µg/mL in PBS, 1hr at 37ºC) for 3 days at 37°C. The Lipofectamine 3000 kit from Invitrogen was used as directed by the manufacturer. siRNA and P3000 reagent were pre-mixed and incubated in Reduced-Serum Medium (Opti-MEM) for 5 minutes at room temperature. In a separate tube, Lipofectamine 3000 was prepared in Opti-MEM. The two mixtures were then combined and incubated at room temperature for 10 minutes to form siRNA-lipid complexes. 200ul of the siRNA/Lipofectamine

complex mix was then added to each well of HUVECs containing 1.8mL normal growth medium.

RNA Extraction

Quick-RNA™ Miniprep Kit from Zymo Research was used for RNA extraction. Samples were first treated with TRIzol (Invitrogen). HUVECs were collected using a plastic cell scraper and the cell suspension was transferred to Eppendorf tubes. Mouse hindbrain tissues were homogenized in TRIzol using 20-gauge syringes through continuous upward and downward movement of the plunger. Samples were then treated with chloroform and centrifuged at 27500 rpm for 15 minutes. Supernatant was collected and mixed well with an equal part of 100 proof ethanol (1:1). The mixture was then transferred to into a Zymo-Spin™ IIICG Column (green) and centrifuged for 30s. Flow-through was discarded. The columns were washed with 400μL RNA wash buffer, then incubated in DNase I for 15min. Afterwards, the samples underwent 1 wash with RNA prep buffer and 2 washes with RNA wash buffer. The sample were then eluted with 30μL DNase/RNase-free water. RNA concentration was measured using NanoDrop® ND-1000 spectrophotometer.

cDNA Preparation and Real-Time Quantitative Reverse Transcription PCR

qScript cDNA SuperMix from Quantabio was used for single-strand cDNA preparation. SYBR Green I dye from KAPA SYBR FAST qPCR Kits (Roche) was added to cDNA samples along with primers. Fold change was calculated using quantification Cq results and the delta-delta Ct method (also known as the $2^{-\Delta\Delta Ct}$ method) and normalized to the expression of GAPDH.

Statistical Analysis

PRISM software (version 9.1.1, GraphPad Software) was used to perform statistical analysis. Data analysis was done using one-way ANOVA with the Bonferroni post-hoc test, as indicated in each figure caption. The resulting P values are indicated as follows: NS, not significant; * $p < 0.05$; ** $p < 0.01$; *** $p < 0.001$

This thesis contains unpublished materials preparing for publication co-authored with McCurdy, Sara; Gingras, Alexandre; Ginsberg, Mark H. The thesis author will be an author of the paper.

REFERENCES

Akers, Amy; Salman, Rustam Al-Shahi; Awad, Isaam A.; Dahlem, Kristen; Flemming, Kelly; Jusue-Torres, Ignacio; Kondziolka, Douglas; Lee, Cornelia; Morrison, Leslie; Rigamonti, Daniele; Rebeiz, Tania; Tournier-Lasserve, Elisabeth; Waggoner, Darrel; Whitehead, Kevin. "Synopsis of Guidelines for the Clinical Management of Cerebral Cavernous Malformations: Consensus Recommendations Based on Systematic Literature Review by the Angioma Alliance Scientific Advisory Board Clinical Experts Panel." *Neurosurgery*, vol. 80, no. 5, 2017, pp. 665–680., doi:10.1093/neuros/nyx091.

Anderson, J. M., and C. M. Van Itallie. "Physiology and Function of the Tight Junction." *Cold Spring Harbor Perspectives in Biology*, vol. 1, no. 2, 2009, doi:10.1101/cshperspect.a002584.

Bazzoni, Gianfranco, and Elisabetta Dejana. "Endothelial Cell-to-Cell Junctions: Molecular Organization and Role in Vascular Homeostasis." *Physiological Reviews*, vol. 84, no. 3, 2004, pp. 869–901., doi:10.1152/physrev.00035.2003.

Chan, Aubrey C.; Li, Dean Y.; Berg, Michel J.; Whitehead, Kevin J. "Recent Insights into Cerebral Cavernous Malformations: Animal Models of CCM and the Human Phenotype." *FEBS Journal*, vol. 277, no. 5, 2010, pp. 1076–1083., doi:10.1111/j.1742-4658.2009.07536.x.

De Kreuk, Bart-Jan; Gingras, Alexandre R.; Knight, James DR.; Liu, Jian J.; Gingras, Anne-Claude; Ginsberg, Mark H. "Author Response: Heart of Glass Anchors Rasip1 at Endothelial Cell-Cell Junctions to Support Vascular Integrity." 2015, doi:10.7554/elife.11394.022.

Dejana, Elisabetta. "Endothelial Cell–Cell Junctions: Happy Together." *Nature Reviews Molecular Cell Biology*, vol. 5, no. 4, 2004, pp. 261–270., doi:10.1038/nrm1357.

Draheim, Kyle M.; Fisher, Oriana S.; Boggon, Titus J.; Calderwood, David A.; "Cerebral Cavernous Malformation Proteins at a Glance." *Journal of Cell Science*, vol. 127, no. 4, 2014, pp. 701–707., doi:10.1242/jcs.138388.

Giannotta, Monica; Trani, Marianna; Dejana, Elisabetta; "VE-Cadherin and Endothelial Adherens Junctions: Active Guardians of Vascular Integrity." *Developmental Cell*, vol. 26, no. 5, 2013, pp. 441–454., doi:10.1016/j.devcel.2013.08.020.

Glading, Angela J., and Mark H. Ginsberg. "Rap1 And Its Effector KRIT1/CCM1 Regulate β-Catenin Signaling." *Disease Models & Mechanisms*, vol. 3, no. 1-2, 2010, pp. 73–83., doi:10.1242/dmm.003293.

Guo, Renyong; Sakamoto, Hiroshi; Sugiura, Shigeki; Ogawa, Minetaro. “Endothelial Cell Motility Is Compatible with Junctional Integrity.” *Journal of Cellular Physiology*, vol. 211, no. 2, 2007, pp. 327–335., doi:10.1002/jcp.20937.

Kleaveland, Benjamin; Zheng, Xiangjian; Liu, Jian J.; Blum, Yannick; Tung, Jennifer J.; Zou, Zhiying; Sweeney, Shawn M.; Chen, Mei; Guo, Lili; Lu, Min-min; Zhou, Diane; Kitajewski, Jan; Affolter, Markus; Ginsberg, Mark H.; Kahn, Mark L. “Regulation of cardiovascular development and integrity by the Heart of Glass-Cerebral Cavernous Malformation pathway.” *Nature Medicine.* 2009 Feb; 15(2): 169–176.

Leblanc, Gabrielle G.; Golanov, Eugene; Awad, Issam A.; Young, William L.; Berg, Mike; Chopp, Michael; Gale, Nicholas W.; Gunel, Murat; Lo, Eng H.; Marchuk, Douglas; Rigamonti, Daniele; Tournier-Lasserve, Elisabeth; Berg, Mike; Blasig, Ingolf E.; Boudreau, Nancy; Chopp, Michael; Gale, Nicholas W.; Ginsberg, Mark H.; Jin, Kunlin; Johnson, Gary L.; Kim, Helen; Lawton, Michael T.; Letarte, Michelle; Li, Dean Y.; Lo, Eng H.; Marchuk, Douglas; Mohr, JP.; Nishimura, Stephen; Noonan, Douglas; Pawlikowska, Ludmila; Plate, Karl H.; Rigamonti, Daniele; Shenkar, Robert; Tournier-Lasserve, Elisabeth; Salman, Rustam Al-Shahi; Ball, Karen L.; Clancy, Marianne S.; Connolly Jr., Sander E.; Derry, Brent; Faurobert, Eva; Gault, Judith; Golanov, Eugene; Hannegan, Lisa; Hashimoto, Tomoki; Keep, Richard F.; Lee, Connie; McCarty, Joseph; Morrison, Leslie; Ning, MingMing; Nunn, Michael F.; Oh, S. Paul; Plahn, Beth K.; Pratt, Charlotte A.; Pratt, Wande B.; Spatz, Maria; Stapf, Christian; Yang, Guo-Yuan; Zhang, Jun. “Biology of Vascular Malformations of the Brain.” *Stroke*, vol. 40, no. 12, 2009, doi:10.1161/strokeaha.109.563692.

Li, Jia; Zhao, Yang; Choi, Jaesung; Ting, Ka Ka; Coleman, Paul; Chen, Jinbiao; Cogger, Victoria C.; Wan, Li; Shi, Zhongsong; Moller, Thorleif; Zheng, Xiangjian; Vadas, Mathew A.; Gamble, Jennifer R. “Targeting MiR-27a/VE-Cadherin Interactions Rescues Cerebral Cavernous Malformations in Mice.” *PLOS Biology*, vol. 18, no. 6, 2020, doi:10.1371/journal.pbio.3000734.

Padarti, Akhil, and Jun Zhang. “Recent Advances in Cerebral Cavernous Malformation Research.” *Vessel Plus*, vol. 2, no. 8, 2018, p. 21., doi:10.20517/2574-1209.2018.34.

Petzelbauer, Peter.; Halama, Thomas; Gröger, Marion. “Endothelial Adherens Junctions.” *Journal of Investigative Dermatology Symposium Proceedings*, vol. 5, no. 1, 2000, pp. 10–13., doi:10.1046/j.1087-0024.2000.00002.x.

Sangwung, Panjamaporn; Zhou, Guangjin; Nayak, Lalitha; Chan, E. Ricky; Kumar, Sandeep; Kang, Dong-Won; Zhang, Rongli; Liao, Xudong; Lu, Yuan; Sugi, Keiki; Fujioka, Hisashi; Shi, Hong; Lapping, Stephanie D.; Ghosh, Chandra C.; Higgins, Sarah J.; Parikh, Samir M.; Jo, Hanjoong; Jain, Mukesh K. “KLF2 And KLF4 Control Endothelial Identity and Vascular Integrity.” *JCI Insight*, vol. 2, no. 4, 2017, doi:10.1172/jci.insight.91700.

Stevenson, B. R.; Siliciano, J. D.; Mooseker, M. S.; Goodenough, D. A.; "Identification of ZO-1: a High Molecular Weight Polypeptide Associated with the Tight Junction (Zonula Occludens) in a Variety of Epithelia." *The Journal of Cell Biology*, vol. 103, no. 3, 1986, pp. 755–766., doi:10.1083/jcb.103.3.755.

Su, Valerie L., and David A. Calderwood. "Signalling through Cerebral Cavernous Malformation Protein Networks." *Open Biology*, vol. 10, no. 11, 2020, p. 200263., doi:10.1098/rsob.200263.

Zheng, Xiangjian; Riant, Florence; Bergametti, Françoise; Myers, Cynthia D.; Tang, Alan T.; Kleaveland, Benjamin; Pan, Wei; Yang, Jisheng; Tournier-Lasserve, Elisabeth; Kahn, Mark L. "Cerebral Cavernous Malformations Arise Independent of the Heart of Glass Receptor." *Stroke*, vol. 45, no. 5, 2014, pp. 1505–1509., doi:10.1161/strokeaha.114.004809.

Zhou, Zinan; Tang, Alan T.; Wong, Weng-Yew; Bamezai, Sharika; Goddard, Lauren M.; Shenkar, Robert; Zhou, Su; Yang, Jisheng; Wright, Alexander C.; Foley, Matthew; Arthur, J. Simon C.; Whitehead, Kevin J.; Awad, Issam A.; Li, Dean Y.; Zheng, Xiangjian; Kahn, Mark L. "Cerebral cavernous malformations arise from endothelial gain of MEKK3-KLF2/4 signaling." *Nature*. 2016 Apr 7; 532(7597): 122–126.

Zhou, Zinan; Rawnsley, David R.; Goddard, Lauren M.; Pan, Wei; Cao, Xing-Jun; Jakus, Zoltan; Zheng, Hui; Yang, Jisheng; Arthur, J. Simon C.; Whitehead, Kevin J.; Li, Dean; Zhou, Bin; Garcia, Benjamin A.; Zheng, Xiangjian; Kahn, Mark L. "The Cerebral Cavernous Malformation Pathway Controls Cardiac Development via Regulation of Endocardial MEKK3 Signaling and KLF Expression." *Developmental Cell*, vol. 32, no. 2, 2015, pp. 168–180., doi:10.1016/j.devcel.2014.12.009.